Implementation and evaluation of a transit dosimetry system for treatment verification

Ricketts, K.[1,2], Navarro, C.[2], Lane, K.[2], Moran, M.[2], Blowfield, C.[2], Kaur, U.[2], Cotten, G.[2], Tomala, D.[2], Lord, C.[2], Jones, J.[2], Adeyemi, A.[2]

[1]Division of Surgery and Interventional Sciences, University College London, London, UK

[2]Department of Radiotherapy Physics, Royal Berkshire NHS Foundation Trust, Reading, UK

Corresponding author: Dr Kate Ricketts: k.ricketts@ucl.ac.uk

Abstract

Purpose: To evaluate a formalism for transit dosimetry using a phantom study and prospectively evaluate the protocol on a patient population undergoing 3D conformal radiotherapy.

Methods: Amorphous silicon EPIDs were calibrated for dose and used to acquire images of delivered fields. The measured EPID dose map was back-projected using the planning CT images to calculate dose at pre-specified points within the patient using commercially available software, EPIgray (DOSIsoft, France). This software compared computed back-projected dose with treatment planning system dose. A series of tests were performed on solid water phantoms (linearity, field size effects, off-axis effects). 37 patients were enrolled in the prospective study.

Results: The EPID dose response was stable and linear with dose. For all tested field sizes the agreement was good between EPID-derived and treatment planning system dose in the central axis, with performance stability up to a measured depth of 18 cm (agreement within -0.5% at 10 cm depth on the central axis and within -1.4% at 2 cm off-axis). 126 transit images were analysed of 37 3D-conformal patients. Patient results demonstrated the potential of EPIgray with 91% of all delivered fields achieved the initial set tolerance level of ΔD of 0 ± 5-cGy or $\%\Delta D$ of $0 \pm 5\%$.

Conclusions: The in vivo dose verification method was simple to implement, with very few commissioning measurements needed. The system required no extra dose to the patient, and importantly was able to detect patient position errors that impacted on dose delivery in two of cases.

1   Introduction

It is now recommended by various national and international organisations that in vivo dosimetry monitoring should be undertaken by each radiotherapy centre [1] [2] [3]. In vivo dose measurements when compared to planned doses can spot errors in patient set-up, data transcription, machine fault or anatomical changes which may lead to over- or under-dosage of the tumour volume and unplanned

toxicity. Point detectors such as diodes and thermoluminescent dosimeters are commonly used for these measurements. However, point detectors are sensitive to positioning errors particularly in highly modulated fields [4]. . Such detectors are placed on external contours of patients, but it is known that external displacements can differ from internal tumour displacements up to approximately 2 cm [5] [6].

Within the radiotherapy physics community EPID dosimetry is widely seen to have the potential to become an accurate and efficient means of large-scale patient specific dose verification [7] [8] [9] [10]. A recent paper reported that between 2005 and 2009 the treatment plans of 4337 patients were verified using in vivo EPID dosimetry, among which 17 serious errors were detected [11]. Of these, 9 would have been missed if no treatment verification had been performed, thereby highlighting the importance of the method.

Current EPID technology for transit dosimetry is based upon passive, amorphous silicon (a-Si) flat panel imagers. Previous approaches have considered CCD camera based systems and liquid filled ionisation chamber matrixes. a-Si has proven popular due to its superior image quality and dose characteristics (linearity, uniformity, dose-rate dependence, field size dependence, relative dosimetry) [12] [13] [14].

Although of great use, EPID in vivo verification technology is still being developed and is not routinely available. A number of departments have implemented in vivo EPID dosimetry using in-house solutions [15], [16], [17] . The availability of a new commercial software EPIgray (DOSIsoft, France) has enabled us to use EPID devices as a portal dosimeter for in vivo dose verification. In this work the algorithm was implemented to calculate the point dose within any pre-specified location(s) within the patient, based on a recent publication which presents a method for back-projection of measured EPID fluence map to the plane of the patient [18]. A series of phantom measurements were undertaken to verify the algorithm's performance under a range of beam conditions. A review board approved study was undertaken at the Royal Berkshire NHS Foundation Trust to prospectively

evaluate the algorithm's performance on a patient population, giving important test conditions that phantom studies cannot (namely anatomical changes including weight loss/gain, organ motion, tumour size changes etc.). This study was used to gain insight into clinical issues that come into play upon clinical implementation of EPID-based in vivo dose verification.

2   Materials and Methods

2.1   Commissioning EPIgray

EPIgray version 2.0.3 software was used along with Elekta Synergy® and Precise linear accelerators running Integrity (Elekta, Crawley, UK) equipped with portal imaging system iViewGT a-Si panels (PerkinElmer, USA), and motorised 60° physical wedge. The sensitive layer consists of 1024 x 1024 pixels with a pitch of 400 µm, resulting in an active area of 409.6 x 409.6 mm^2 [19]. All measurements were performed with a nominal dose rate of 400 MU/min. Three linear accelerators were used for the patient measurements: the machines were matched to within Elekta specifications; for photons this is 1% for depth doses and output factors and 2% for profiles, although for most of the tested clinical fields upon commissioning, the match was found to be better than this. The treatment planning system (TPS) was Eclipse version 10.0 (Varian MS, Palo Alto, USA) with Analytic Anisotropic Algorithm (AAA). IMPAC/Mosaiq record and verify system version 2.41 (Elekta, Crawley, UK) was used to transfer plan parameters to the linear accelerator control system. Image datasets of patients and phantoms used were acquired with a GE LightSpeed 16 CT Scanner.

Prior to EPIgray commissioning the EPIDs were prepared for dosimetric measurement, according to manufacturer guidelines to ensure that all pixels have a similar response to a given irradiation and mechanical accuracy within 1 mm. The dosimetric properties of iViewGT EPIDs have been extensively investigated elsewhere [20].

The commissioning of EPIgray required configuration data for the CT, linear accelerator and EPID device. The HU to electron density calibration curve of the CT scanners was required. In order to model the linear accelerator the following were incorporated into the EPIgray beams library for each energy: beam profiles, percentage depth dose and quality index of open and wedged fields. A 10 x 10 cm^2 calibration image was taken for each energy with zero phantom thickness (through the treatment couch) for 100 MU to obtain a calibration factor (CF) that converted EPID signal to dose in water. A diagonal dose profile was input into the beams library to perform an equalisation correction for the EPID image, and linearity correction factors calculated to correct the nonlinearity of the EPID with MU variation. EPID measurements were performed to acquire linearity factors at 10 – 500 MU, 10 x 10 cm^2 field, zero phantom thickness and calculated as:

$$Correction_{MU} = \left[\frac{image\,value_{MU}}{image\,value_{100\,mU}} \right] \times \left[\frac{100\,MU}{MU} \right] \qquad (1)$$

Couch transmission correction was commissioned per manufacturer guidelines which involved (i) measurement of an open field at 0 gantry angle through 20 cm thick solid water, (ii) measurement of the same field through the same phantom thickness at 90 gantry angle. The latter measurement provided a couch transmission value through the entire width of the couch. An average couch transmission factor derived by the manufacturer from data from (i) and (ii) was applied to all 3D conformal fields as per the EPIgray algorithm.

Finally, finite Tissue Maximum Ratio (fTMR) measurements were acquired and input into the EPIgray library, as guided by the manufacturer. fTMR is the ratio between two doses measured in a phantom at d_{max}. The numerator is the dose measured in the presence of an absorber of thickness 't' and the denominator is the dose measured in the same conditions without an absorber [18]. fTMR is measured in the presence of an absorber of finite thickness as opposed to TMR where the phantom

dimensions are infinite. Commissioning fTMR measurements consisted of ion chamber dose measurement at source to chamber distance of 160 cm (at EPID position) within a water tank at depth d_{max} for each energy. fTMR measurements were performed for three overlying absorber solid water set-ups: with SAD of 100 cm to (i) top, (ii) centre and (iii) bottom of the solid water. Commissioning measurements were over five square field sizes (2 x 2 cm^2 - 25 x 25 cm^2), each for six solid water thicknesses (0 - 40 cm) across the three aforementioned solid water SDDs. In addition EPID images were acquired at each solid water / field size / energy configuration for set up (ii).

For all EPID images a dicom image and log file were needed; the latter provided the pixel scaling factor (PSF) for each image; this value held the dosimetric information of the pixel values, as iViewGT performed a greyscale normalisation to ensure that an image acquired with 5 MU has approximately the same grey level as a 500 MU image. Un-normalised pixel values s(x,y) were obtained from normalised values (s*(x,y)) as in Equation 2:

$$s(x, y) = \frac{(2^{16} - 1) - s*(x, y)}{PSF} \qquad (2)$$

2.2   EPIgray Dose Calculation Process

The calibration factor CF measured during commissioning converted EPID dose to dose in water at d_{max}. Dividing by the appropriate finite tissue maximum ratio (fTMR) removed the effect of the overlying patient. Within the software fTMR values were expressed in a look up table of coefficient values listed for patient thickness (5 – 40 cm), field size defined at the EPID (3.2 x 3.2 cm to 40 x 40 cm). An inverse square law correction was then used to recover dose at the position of the pre-specified dose calculation point P (at depth of maximum dose d_{max}) from dose at the EPID (SDD = 160 cm). A TMR correction shifted the reconstruction point from d_{max} to point P. The fluence matrices for TMR and fTMR were calculated by individually computing the primary and scatter component. The primary component was yielded by attenuation correction of the fluence matrix

(modelled using PDD and fluence profile) using attenuation coefficients derived from the quality indices provided during commissioning. The software contained a look up table of computed scatter factors as a function of field size of subsector and depth of point P. Peak scatter factor (PSF) values set within the software data tables were used to calculate the overall scatter factors; PSF describes dose to scatter only (defined as: dose in tissue at d_{max} / dose at d_{max} due to primary radiation only). PSF values for our centre were provided by the manufacturer and obtained from the quality indices of each beam energy provided during commissioning. The algorithm divided each field into subsectors, and the scatter table searched using depth and field size for each subsector. Scatter values of each subsector were then summed.

CT images were acquired of the phantoms and patients and exported to the TPS in which a dose distribution was calculated over the set MU and field configurations. Reference dose calculation points were created within the TPS; it is to these predefined points that EPIgray reconstructs the dose and compares to TPS calculated dose. For phantom studies, a number of reference points were used to build up beam profiles and depth doses for EPIgray-TPS comparison.

The CT images, structures, RTPlan file and dose matrix were exported from the TPS to the EPIgray console. Validated treatment plans were exported to the record and verify system (Mosaiq) to enable treatment geometries to be reproduced and delivered by the accelerator. Treatment fields were delivered and MV portal images were acquired during treatment in single shot mode for 3D conformal fields. The appropriate iView image dataset was queried by the EPIgray software, and dose to the pre-specified reference point was calculated using the EPIgray software algorithm [21]. EPIgray automatically calculated the percentage difference between EPID-derived dose (D_{EPI}) and TPS-calculated dose (D_{TPS}), (%Δ_D, Eq 3) and used this value to either pass or fail the measurement according to thresholds preset by the user. The software had no function to automate and set thresholds on absolute dose difference ($\mathbf{\Delta_D} = D_{EPI}-D_{TPS}$), and so $\mathbf{\Delta_D}$ values were manually calculated in this study.

$$\%\Delta_{D} = (D_{EPI}\text{-}D_{TPS})/D_{TPS}\ (\%) \qquad (3)$$

2.3   Phantom measurements

The following measurements were undertaken using a 20 cm thick solid water phantom (25 x 25 cm) set at 90 cm SSD at 6 MV and 10 MV unless otherwise specified. A number of isocentric and off-axis reference points were created within the TPS, and D_{EPI} was compared to D_{TPS} for each reference point.

The reproducibility of the EPID devices were measured across ten repeat deliveries of a 10 x 10 cm^2 field delivering 100 MU across different days over a one month period at 6 MV and 10 MV. The linearity of dose response was tested: over 5 - 200 MU, field size 10 x 10 cm, at the isocentre. Field size dependence was tested for three open field sizes (5 x 5, 10 x 10, 15 x 15 cm) each exposed to 100 MU. Three dose reconstruction points were defined in the TPS: (i) 5 cm depth on central axis (cax), 10 cm depth on the central axis, 5 cm depth and 2 cm off axis. Off-axis dose calculation was tested: A 20 x 20 cm field was delivered (100 MU) and 21 dose reconstruction points were created (in 1 mm increments near field edge and 10 – 15 mm increments in field centre) across the beam profile at two different depths (5 cm and 10 cm deep). The effect of depth of reconstruction point P was investigated: a 10 x 10 cm field (100 MU) was delivered at a range of SSDs (80, 90 and 100 cm SSD). Dose reconstruction points were created on the central axis at depths 1 – 18 cm in 1 cm increments. Dose calculation of wedged fields was measured: A 20 x 20 cm fully wedged field (100 MU) was delivered and dose reconstruction points were created in 10 mm increments across the beam profile at depth 5 cm to assess beam profile modelling, and at depths 1 – 18 cm on the central axis to assess depth effects.

Additional tests were performed to assess the sensitivity of EPIgray to detection of errors in (i) SSD, and (ii) patient thickness. (i) A 10 x 10 cm field (100 MU) was planned at 90 cm SSD, 20 cm thick solid water. The field was delivered with induced errors in SSD (80 – 100 cm SSD in 5 cm increments). (ii) The previous plan was delivered to (a) 10 cm, (b) 20 cm and (c) 30 cm thick solid

water (matching the plan), and errors in patient thickness induced by varying the water thickness up to $\pm$ 4 cm (keeping the SSD constant at 85 cm for 30 cm thickness, 90 cm for 20 cm thickness, and 95 cm for 10 cm thickness). The ability of EPIgray to detect both errors (i) and (ii) was evaluated through inspecting automatically calculated %Δ_D.

EPIgray performance with heterogeneity was investigated using a phantom designed by the IPSM Radiotherapy Topic Group, made of epoxy resin water equivalent material with an 8 cm diameter cylindrical lung equivalent insert of electron density 0.25 compared with water [22]. A 10 x 10 cm^2 field was delivered at 6 MV and 10 MV with the central axis centred on the lung insert. The central axis of the beam traversed 1.7 cm solid water, 8 cm lung insert and finally 14.3 cm solid water. Dose was reconstructed along the central axis at (i) the centre of the lung insert, and (ii) at an additional 5 cm depth within the solid water portion proximal to the lung insert.

2.4 Patient study

37 patients (2 abdominal, 10 brain, 5 head and neck, 4 lung, 3 pelvis, 10 rectal and 3 sarcoma patients) were included in this study. 119 first fraction iView images and additional 7 repeats were acquired and processed.

All patients were treated supine with the exception of rectal patients who were prone. Brain and head and neck patients were immobilised using a thermoplastic shell. Sarcoma patients were immobilised using vacuum bags. Lung patients were immobilised using wingboards. Each patient setup was verified and corrected using CBCT except for rectal patients who were MV imaged for setup. All pelvis patients were treated with a full bladder apart from the bladder patient who had an empty bladder.

The dose reconstruction point was placed at the isocentre for all plans: this was to mirror previously used diode positions and to profit from the better performance of EPIgray on the central axis. We

used a preliminary action level of $0 \pm 5\%$ and 0 ± 5-cGy for $\%\Delta_D$ and Δ_D respectively, based upon results from a different group [15].

3 Results

3.1 Phantom studies

EPIgray dose calculation was found to have a day to day reproducibility of 0.5% and 0.6% for 6 MV and 10 MV respectively (quoted at the 1-sigma level), with mean $\pm$ 1 SD $\%\Delta_D$ values of ten identical open fields of -0.23% $\pm$ 0.48% and -0.90% $\pm$ 0.64%. EPIgray dose calculation was found to agree well with TPS dose calculation on the central axis over a range of MU (5 – 200 MU) for both 6 MV and 10 MV (Figure 1) with a maximum $\%\Delta_D$ of -1.9%.
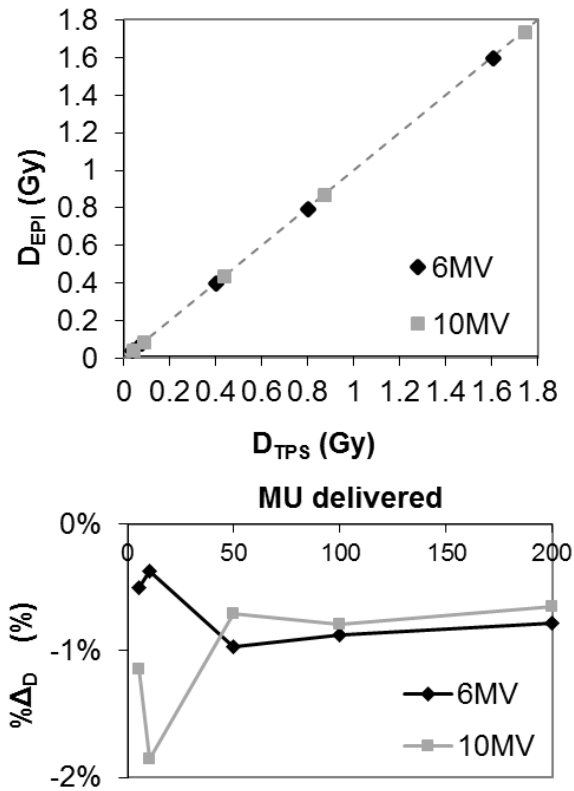
Figure 1 (top) EPIgray and TPS reconstructed doses for delivered monitor units 5, 10, 50, 100, 200 MU, reconstructed at a point 10 cm deep on cax within a 20 cm solid water phantom. Dashed line represents equal EPIgray and TPS reconstructed dose, (bottom) %Δ_D of cax dose reconstruction points at a range of delivered MU at 6 and 10 MV.

Field size was found to have little effect on %Δ_D for dose reconstruction points on the central axis (P1 and P2 within Table 1) for the tested field sizes (5 x 5 - 15 x 15 cm^2). Smaller field sizes show greater difference between D_{EPI} and D_{TPS} for off-axis dose calculation points, as the dose point lies closer to the field edge; dose calculated to a point 2 cm off-axis showed a %Δ_D of +1.9% and +4.3% at 5 x 5 cm^2 field size, 2.4 and 3 times greater than the worse performing on-axis dose calculation for the larger fields at 6 and 10 MV respectively.

Table 1 %Δ$_D$ of a range of field sizes (5 x 5 – 15 x 15 cm^2) delivered to a 20 cm thick solid water phantom set at 90 cm SSD, 100 MU at 6 MV and 10 MV. Dose was calculated at three different reference points: P1 (cax, 5 cm depth), P2 (cax, 10 cm depth), P3 (2 cm off axis, 5 cm depth).

	5 x 5 cm^2			10 x 10 cm^2			15 x 15 cm^2		
	P1	**P2**	**P3**	**P1**	**P2**	**P3**	**P1**	**P2**	**P3**
6MV	-0.1%	0.0%	1.9%	0.0%	-0.1%	-0.5%	-0.6%	0.0%	-0.8%
10MV	-0.4%	-0.5%	4.3%	-0.5%	-0.6%	-1.4%	0.2%	0.3%	-0.7%

Table 2 presents a series of measurements which demonstrate that EPIgray performed well near the central axis (%Δ$_D$ values within -0.5% on the central axis and within -1.1% at 2 cm off-axis measured at 10 cm depth). Off-axis dose points showed greater values of %Δ$_D$ up to -6.4% at 8 cm off-axis. Agreement between D$_{EPI}$ and D$_{TPS}$ worsened at shallower depths: %Δ$_D$ increased by approximately 0.4% when reconstructing dose to a point 5 cm deep compared to 10 cm deep. Points reconstructed at d$_{max}$ demonstrated the greatest values of %Δ$_D$.

Figure 2 shows good agreement between D$_{EPI}$ and D$_{TPS}$ up to a measured depth of 18 cm at each tested SSD for both 6 and 10 MV; all depths beyond the build-up region displayed **%Δ$_D$** within -1.4%, and within -2.2% for shallower regions less than 2 cm deep. EPIgray overestimated dose at depth for 100cm SSD, 10MV by on average 0.3%; this may be attributed to the reported over-sensitisation of EPIDs to lower energy scattered x-rays resulting from the shorter distance between the phantom and the EPID at higher SSDs [18].
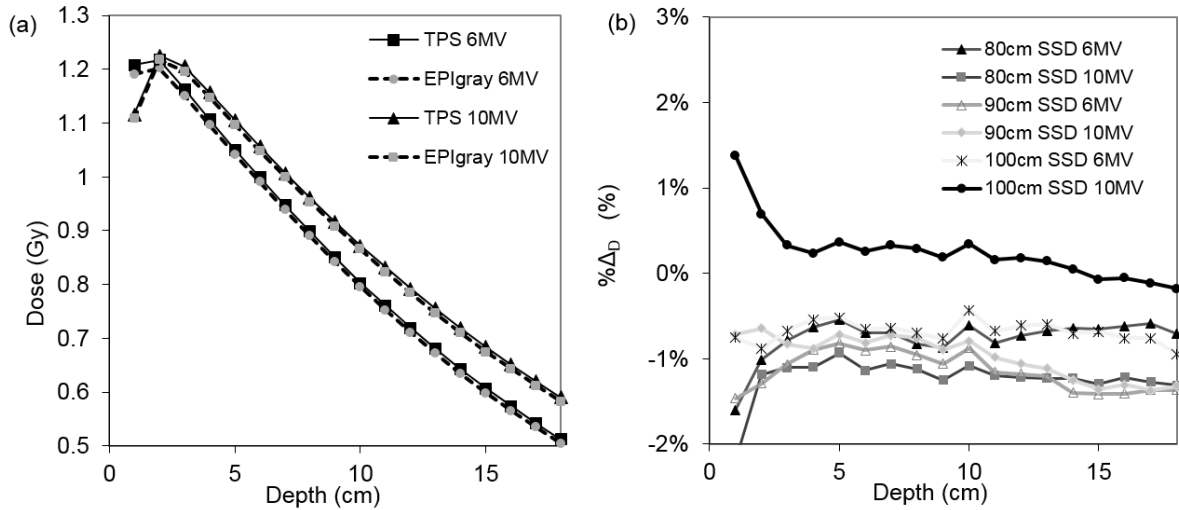
Figure 2 (a) EPIgray and TPS reconstructed doses over a range of depths along the cax: 10 x 10 cm²

field (100 MU, 6 MV and 10 MV) delivered to a 20 cm thick solid water phantom at 90 cm SSD, (b)

%Δ_D of reconstructed doses at a range of depths measured at 80 cm, 90 cm and 100 cm SSD.

Table 2 %Δ_D of reference points calculated across a 20 x 20 cm² field delivered to 20 cm thick solid

water (100 MU). Dose was reconstructed across the beam profiles of depth 10cm, 5 cm and at d_{max},

for 6 MV and 10MV.

	10cm depth		5cm depth		dmax	
	6MV	**10MV**	**6MV**	**10MV**	**6MV**	**10MV**
cax	-0.5%	-0.3%	-0.9%	-0.5%	-1.4%	-0.7%
2 cm off-axis	-1.0%	-1.1%	-1.4%	-1.2%	-1.8%	-1.2%
4 cm off-axis	-2.4%	-3.0%	-3.0%	-3.3%	-3.5%	-3.4%
8 cm off-axis	-6.4%	-5.6%	-7.6%	-5.8%	-8.5%	-5.7%
1 cm from field edge	-16.5%	-8.9%	+17.8%	-11.0%	-13.7%	-8.2%

Figure 3 demonstrated poorer performance of EPIgray for wedged fields than open fields at the tested 90 cm SSD for both 6 and 10 MV, and better modelling of 10 MV than 6 MV. All central axis dose points across measured depths up to 18 cm deep (excluding the build-up region) displayed a **%Δ_D** within -6.9% and -2.8% for 6 and 10 MV compared to -1.4% for the open 20 x 20 cm^2 field. A closer agreement between D_{EPI} and D_{TPS} can be seen at the thick end of the wedge, and for 10 MV compared to 6 MV (Figure 3). As in the case of open fields, dose reconstruction points positioned significantly off-axis towards the thin end of the wedge showed poorer agreement with TPS doses, but better agreement at 6 MV towards the thick end of the wedge (within -2.5% between -6 cm to -9 cm off axis in thick edge direction).
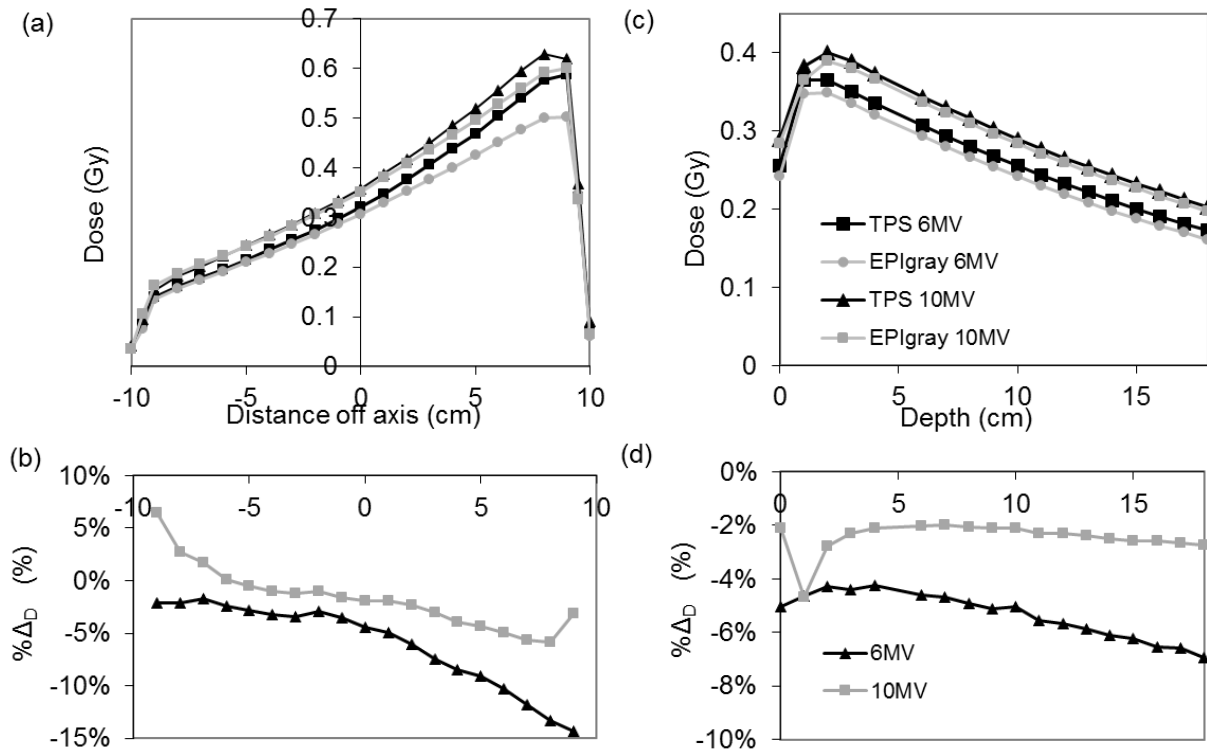

Figure 3 (a) EPIgray and TPS off axis dose reconstruction for 20 x 20 cm fully wedged beam, 100 MU, 90 cm SSD, measured at 6MV and 10 MV at 10 cm depth within solid water (thin edge in positive off-axis direction (b) %Δ_D of off axis dose reconstruction for wedged fields, (c) EPIgray and TPS reconstructed doses over a range of depths along the cax: 20 x 20 cm^2 fully wedged field (100 MU, 6MV and 10MV) delivered to a 20 cm thick solid water phantom at 90 cm SSD, (d) %Δ_D of reconstructed doses at a range of depths for the wedged field.

EPIgray was found to overestimate dose in low density regions compared to TPS calculation; dose calculation discrepancies %ΔD (ΔD) of +3.2% (3.3 cGy) and +4.2% (4.2 cGy) were found within the centre of the lung insert for 6 MV and 10 V respectively. Closer agreement was found within the solid water portion of the phantom: dose discrepancies %ΔD (ΔD) of -2.1% (-1.6 cGy) and -2.2% (-1.6 cGy) were found were found within the solid water region 5 cm proximal to the lung insert for 6 MV and 10 V respectively. Figure 4 demonstrates a marked difference between EPIgray and TPS reconstructed doses at the heterogeneous boundaries between the lung insert and solid water. All %ΔD values were within +5.1%.
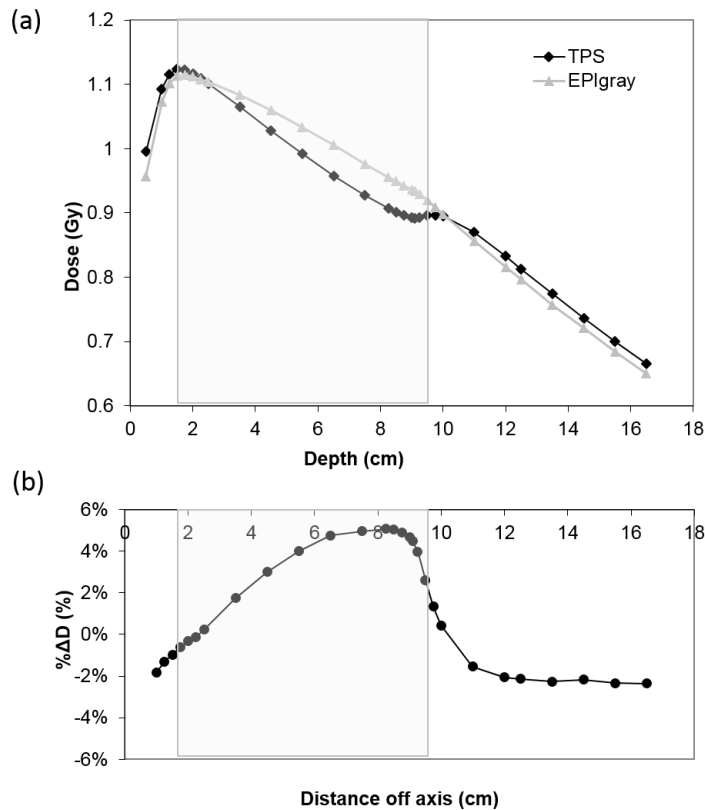

Figure 4 EPIgray and TPS dose reconstruction at depth within the IPSM phantom for 10 x 10 cm open beam, 90 cm SSD, measured at 6MV and 10 MV along the central axis; (b) %Δ$_D$ of dose reconstruction at depth in the IPSM phantom. The shaded region corresponds to the low density lung insert region.

3.2   Sensitivity to errors

A range of errors in phantom thickness were induced from planned phantom thicknesses of 10cm, 20 cm and 30 cm. EPIgray was sensitive to patient separation changes: a reduction in patient separation by 2 cm resulted in **%Δ_D** values of 9.6% (7.6%), 8.5% (6.5%) and 6.1% (5.1%) for a planned patient thickness of 10 cm, 20 cm and 30 cm respectively at 6 MV (10 MV). Likewise an increase in patient separation by 2 cm resulted in **%Δ_D** values of -9.3% (-6.7%), -8.7% (-6.9%) and -9.6% (-7.1%). Errors of 1 cm water equivalent path length resulted in a **%Δ_D** value within tolerance ($\leq$ 5%) for each of the three planned thicknesses and so would not have been detected. Results for each phantom thickness are presented in Figure 5(a) and (b).

On delivering a 10 x 10 cm^2 field to a 20 cm thick solid water phantom over a range of incorrect SSDs different from the planned SSD of 90 cm, it was found that a ~10% error in SSD equated to a difference of ~2% in **%Δ_D** (Figure 5 (c)). EPIgray, and transit dosimetry in general, is not sensitive to errors in SSD, and an additional SSD check should be in place.
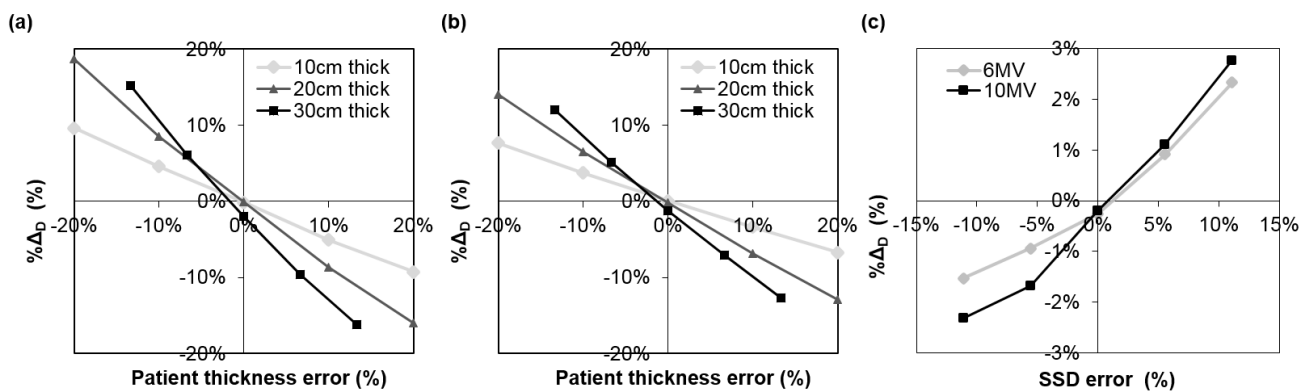

Figure 5 The effect of error in phantom thickness on reconstructed dose presented as percentage difference between EPIgray and TPS calculated dose %Δ_D for three phantom thickness (10 cm, 20 cm and 30 cm) at (a) 6 MV and (b) 10 MV. Phantom thickness error = (treated thickness – planned thickness)/ planned thickness; (c) effect of error in SSD on reconstructed dose presented as

percentage difference between EPIgray and TPS calculated dose %Δ_D. SSD error = (treated SSD –

intended SSD)/ intended SSD, where the intended SSD was 90 cm.

3.3 Patient study

126 images were acquired and analysed across the recruited 37 patients. Table 3 lists the patient demographics. Seven fields could not be measured with EPIgray due to a large floor twist obstructing EPID panel extension (superior anterior oblique fields for seven brain patients). Diode measurements were made of these fields.

The EPID verification model agreed well with TPS dose for 3D conformal fields (Figure 6); a mean of -0.9% lower than D_{TPS} for all fields. Values of %Δ_D and Δ_D for all fields measured for each treatment site are presented in Table 4. Measurements with imager problems were excluded from analysis.

The distribution of percentage (%Δ_D) and absolute ($\Delta_D = D_{EPI} - D_{TPS}$) dose difference for all 126 fields is presented in Figure 7: Δ_D displayed a tighter distribution than %Δ_D. The mean difference between EPID and TPS doses was found to depend on treatment site: ranging from lung which displayed a mean 3.0% overestimation of dose compared to TPS dose, to sarcoma which was on average -3.9% less than TPS dose. Head and neck patients displayed the greatest standard deviation in %Δ_D followed by lung patients (SD of 6.6% and 5.4% respectively) whereas brain and pelvic patients displayed a lower standard deviation of 2.6% and 2.5% respectively. Results for each treatment site are displayed in Table 4.

Wedged fields delivered to patients performed well: all wedged fields were analysed together and displayed an average %ΔD value of -0.5 ± 5.4% compared to -1.7 ± 4.7% for all open fields. Upon excluding patients with high levels of heterogeneity (lung and head and neck fields) the %ΔD values of wedged and open fields came to a closer agreement (-2.1 ± 3.9% and -2.3 ± 4.6% respectively).

7 image repeats were acquired and processed due to the following reasons for initial failure: (i) one left bicep which appeared to have a small amount of rotation of the arm upon inspecting iView versus digitally reconstructed radiograph verification images; (ii) one axilla sarcoma which failed due to the presence of a couch bar attenuating the exit beam, (iii) one rectum failed due to patient position, (iv) three due to imager failure, and (v) one larynx field failed also on repeat due to a large amount of air in the beam path and the failed field was re-measured with a diode and passed. In addition patient 18 was re-planned due to tumour shrinkage. For this patient two out of three fields failed on fraction 1: $\%\Delta_D$ (Δ_D) of 10.9% (9.6 cGy) and 10.1% (8.1 cGy) respectively; due to the irregular tumour shape the isocentre was out of tumour and not placed in soft tissue. Throughout the course of treatment the tumour shrank and became more regular which enabled a simpler plan with isocentre placed within the tumour soft tissue. All three fields passed on the first verification of the replan: $\%\Delta_D$ (Δ_D) of 5.6% (3.3 cGy), 5.0% (4.9 cGy) and 1.2% (1.5 cGy).

Table 3 Demographic information for the 37 patients enrolled on the study

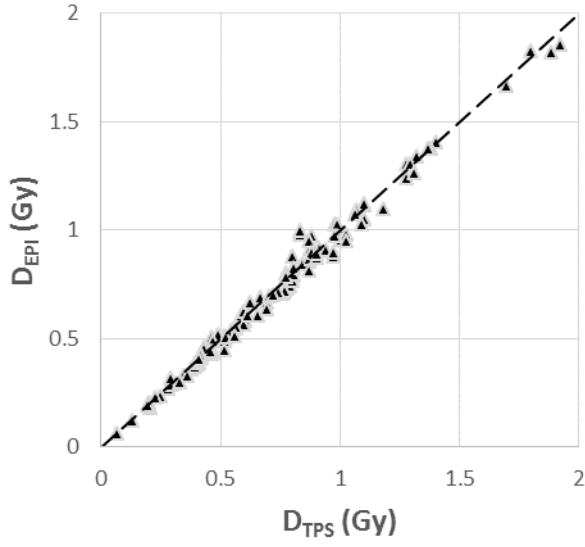| Patient Number	Anatomic site	Fields per patient (Energy)	No. open (wedged) fields
1	Abdomen	3 (6 MV)	0 (3)
2	Pancreas	3 (10 MV)	0 (3)
3 – 12	Brain	2-5 (6 MV)	0 (25)
13 – 16	Larynx	2-3 (6 MV)	1 (10)
17	Oesophagus	4 (10 MV)	1 (3)
18a	Right lung	3 (10 MV)	0 (3)
18b	Right lung re-plan	3 (10 MV)	1 (2)
19-21	Left lung	3-4 (10 MV)	0 (10)
22	Bladder	3 (10 MV)	1 (2)
23-24	Endometrium	4 (10 MV)	3 (5)
25 – 34	Rectum	3-4 (6 and 10 MV)	11 (26)
35	Sarcoma Lt bicep	3 (6 MV)	1 (2)
36	Sarcoma Right flank	3 (6 and 10 MV)	1 (2)
37	Sarcoma Axilla	3 (6 and 10 MV)	3 (0)

Figure 6 D_{EPI} and D_{TPS} reconstructed doses of each measured patient field for 126 3D conformal beams. Dashed line: $D_{EPI} = D_{TPS}$
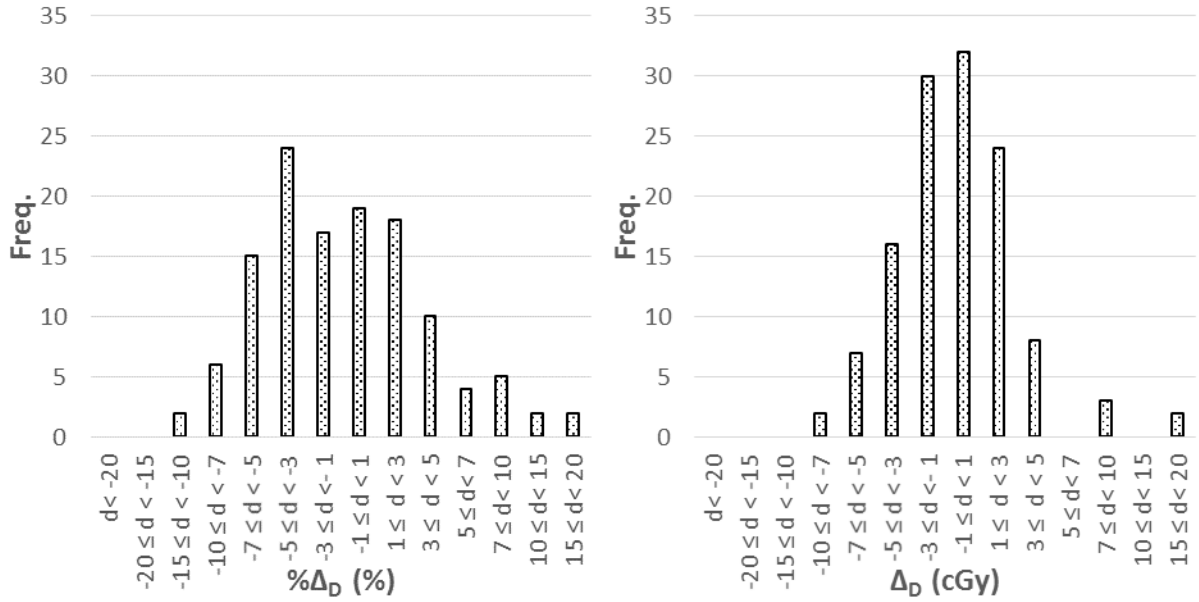

Figure 7 Histograms of $\%\Delta_D$ and Δ_D of 126 patient-delivered 3D conformal fields

Table 4 Summary of results of EPID patient transit dosimetry; %Δ_D and Δ_D values for all measured fields per site, pass / fail status of fields and reasons for failure

Site	Patient number	No. fields measured	%Δ_D ± 1 SD	Δ_D ± 1 SD (cGy)	Pass / fail status	Reason for fail
Abdomen	1,2	6	1.0 ± 2.1	1.1 ± 1.8	All pass	
Brain	3-12	25	-3.2 ± 2.6	-2.0 ± 1.8	All pass	
Head and neck	13-17	16	2.0 ± 6.6	1.4 ± 5.1	1 field failed; Repeat failed	Ray trace passed significant amount of air
Lung	18-21	16	3.0 ± 5.4	2.1 ± 4.3	Patient 19 (2 fields) failed; Patient 19 re-planned and passed	Isocentre in heterogeneity. Replan: Isocentre in soft tissue
Pelvis	22-24	13	-3.5 ± 2.5	-2.6 ± 1.7	2 fails, passed upon repeat	2 x Imager malfunctions
Rectum	25-34	40	-0.9 ± 4.9	-0.3 ± 2.4	1 fail, passed upon repeat; 1 fail, passed upon repeat	Patient positioning error Imager malfunction
Sarcoma	35-37	10	-3.9 ± 4.1	-3.0 ± 3.7	1 fail, passed upon repeat; 1 fail, passed upon repeat	Unplanned arm rotation Attenuation of exit beam by immobilisation device
All wedged		103	-0.5 ± 5.4	-0.2 ± 3.9		
All open		23	-1.7 ± 4.7	-1.1 ± 3.1		
All wedged		75	-2.1 ± 3.9	-1.3 ± 2.6		
All open (excluding lung / H&N)		20	-2.3 ± 4.6	-1.6 ± 2.9		
All	**1-37**	**126**	**-0.9 ± 5.0**	**-0.4 ± 3.4**	**7 image repeats (including 3 imager problems); 1 re-plan**	

4 Discussion

A series of phantom measurements demonstrated that EPIgray performed well near the central axis (%Δ_D values within -0.5% at 10 cm deep), with performance stability up to a measured depth of 18 cm excluding the build-up region (%Δ_D values within -1.4%). Doses calculated on the central axis were found to be unaffected by field size (across measured field sizes 5 x 5 and 20 x 20 cm^2) and good performance observed across a range of MU (stable within the tested 5 – 500 MU). EPIgray was

found to be reasonably sensitive to patient thickness changes but unable to reliably detect thickness changes of less than 1 cm. EPIgray was not sensitive to SSD errors (Figure 5); the latter is common to all transit dosimetry [16].

Wedged fields were found to be modelled less well within the phantom study (central axis $\%\Delta_D$ values were within -4.5% at 10 cm deep and within -6.9% up to a measured depth of 18 cm excluding the build-up region). In addition, the dose to off-axis points (> 2cm off-axis) or points within 1 cm of the field edge had a greater $\%\Delta_D$ value than central axis points in all cases. This corroborates well with previous TPS commissioning measurements: agreement between the TPS and machine delivery was measured using ion chambers and a 2D array across a range of open field parameters and was within ± 2% for the majority of the points tested. However, for a number of off-axis, wedged and wedged off-axis points ion chamber measurement was found to be up to 3% less than TPS dose. It is therefore recommended that dose points are created on the central axis or within 2 cm of the central axis where possible.

In order to test EPIgray performance with heterogeneity we measured 126 beams delivered to a cohort of 37 patients comprised of abdominal, brain, head and neck, lung, pelvis, rectal and sarcoma 3D conformal treatments. Patient results demonstrated the potential of EPIgray to verify delivered dose well within inhomogeneities; 91% of all delivered fields achieved the initial set tolerance level of Δ_D of 0 ± 5 cGy or $\%\Delta_D$ of 0 ± 5%. In addition a short study using an inhomogeneous phantom containing an 8 cm diameter cylindrical lung equivalent insert demonstrated that EPIgray overestimated dose within low density regions, by up to $\%\Delta_D$ of +5.1%. However dose reconstruction points were not placed within heterogeneities within the patient trial. Nevertheless dose reconstructed in solid water regions distal to the lung insert displayed $\%\Delta_D$ values up to -2.4%; when compared to central axis measurements measured up to 18 cm depth within homogeneous phantoms (which yielded $\%\Delta_D$ within -1.4%) it is evident that heterogeneity within the beam path affects Epigray performance.

Importantly the system was able to detect errors in patient set up; patient 35 (left bicep) had a small amount of rotation of the arm in the first measurement as noted from verification images. On the repeat the expected and measured iView images coincided well and the field passed. This is a common issue for treatment of sarcomas in our centre as vacuum bags are used for immobilisation, and are less reproducible than thermoplastic shells. Patient 26 was found to have shifted on the order of 2 mm upon inspection of verification images; this translated to a $\%\Delta_D$ (Δ_D) value of the posterior field of -12.5% (-6.4 cGy) for this fraction due to a highly modulated patient surface overlying the dose calculation point. On the repeat the verification images coincided well with planned images and the field passed ($\%\Delta_D = 4.5\%$).

Other than patient errors, a number of factors also contributed to out of tolerance measurements for this measured cohort including: (i) EPID imager malfunction for 3 fields; (ii) Attenuation of the exit beam through devices, e.g. the couch bar present for patient 37. Such devices are accounted for in the TPS only for devices proximal to the beam entrance; (iii) Algorithm limitations: The TPS AAA algorithm and EPIgray algorithm deal with tissue heterogeneity differently.

The standard deviation of $\%\Delta_D$ varied with treatment site, and indicated the stability of conditions through which the central axis ray line traversed. Head and neck and lung fields showed the greatest standard deviations (6.6% and 5.4% respectively), due to (i) tissue heterogeneity (and thus sensitivity to slight changes in patient position), and (ii) including regions of potential anatomical change. Brain is a more homogeneous site suffering less anatomical change and thus displayed a lower standard deviation of 2.6%.

Wedged fields delivered to patients performed well: all wedged fields were analysed together and displayed an average $\%\Delta D$ value of -0.5 ± 5.4% compared to -1.7 ± 4.7% for all open fields. Upon excluding patients with high levels of heterogeneity (lung and head and neck fields) the $\%\Delta D$ values of wedged and open fields came to a closer agreement (-2.1 ± 3.9% and -2.3 ± 4.6% respectively). It was expected that patient wedged fields performed better than the phantom results because the latter

displayed results of a fully 60° wedged field, whereas patient fields generally had a lower wedge weighting. Wedged fields delivered to patients corroborated well with results for wedged fields within the phantom study, which found that central axis dose was in closer agreement to TPS for 10 MV fields than 6 MV fields (%ΔD = -4.5% and -1.9% for 6 MV and 10 MV beams respectively). A greater deviation from TPS dose was found for 6 MV patient wedged fields compared to 10 MV: %Δ_D of -2.7 ± 3.1% and -0.9 ± 4.8% respectively, analysed for all patients excluding head and neck and lung in order to reduce heterogeneity to closer model phantom conditions.

EPIgray tended to overestimate dose compared to TPS for treatment sites that involved beam transit through low density such as lung and head and neck (mean %Δ_D of 3.0% and 2.0% respectively). Other sites displayed an underestimation of dose compared to TPS, such as pelvis, brain and sarcoma (mean %Δ_D of -3.5%, -3.2% and -3.9% respectively), whereas the solid water phantom study predicted better agreement (%Δ_D values within -0.5% at 10 cm deep). This can be attributed to the difference in handling heterogeneity between the EPIgray algorithm and the TPS AAA algorithm. For this reason it may be important to consider setting asymmetric action levels, different for each treatment site, but no firm action levels could be set from this data as more patient numbers would be required.

Transit dosimetry cannot be used for all patient treatments: within this cohort 7 fields could not be measured due to inability to extend the EPID, and diode measurements were made of these fields. We suggest the following patient exclusion criteria: (1) Patients requiring a floor twist, table lateral setting or immobilisation device that impedes panel extension, (2) patients with superior anterior oblique fields which impede panel extension, as evident in this cohort, (3) field lengths greater than 26 cm with a collimator twist. The latter is in place to reduce irradiation of EPID panel electronics, which can shorten the lifetime of the EPID. In addition there are cases where the isocentre is placed in the patient centre even for peripheral targets to ensure that CBCT or arc therapy gantry motion is possible without collision. For such cases off-axis dose calculation is

required to enact treatment verification, and so further improvement to off-axis modelling would be beneficial to ensure EPIgray can be used in these cases.

We have found that the pass / fail status of a field was influenced by the location of the dose calculation point. Other groups have chosen points on the central axis at 5 cm deep [15] [16]; however we decided to position our points at isocentric depth for dose calculation at tumour position, and Figure 2 displayed that EPIgray performance was stable up 18 cm depth as measured in a water phantom. From the phantom measurements we recommend that the dose reference point should be placed at the isocentre (the protocol we have adopted in our centre), or in a position that meets the following criteria in order to reduce false positives: (i) lies > 2 cm from a field edge, (ii) lies < 2 cm from the central axis, (iii) must not lie in a high dose gradient, (iv) must not lie in a low dose area (< 90% of prescribed dose), (v) must not lie beneath MLCs, this may not be avoidable for some IMRT segments but should be minimised as much as possible, or (vi) avoid positions where a slight change in lateral or sup-inf position of the point results in a large change of geometrical or radiological depth (i.e. regions of highly modulating surface contour or heterogeneity along the field projection), (vi) must not lie in air. Points (i), (ii), (iii) and (v) may have implications for small field segments in IMRT fields, by an amount related to the weighting of such small segments. However another group has demonstrated promising results for the use of EPIgray to measure IMRT fields of head and neck patients (mean ± 1SD of %ΔD 1.53% ± 2.46%) and stated that field fails were mainly due to the dose calculation point lying within high dose gradient regions [21]. Testing EPIgray performance for these more complex fields is currently being undertaken at our centre.

There is a required difference between how the TPS and EPIgray must deal with couch attenuation. TPS requires a couch attenuation factor for fields that pass the couch proximal to the patient (which affects patient dose). Transit dosimetry requires a couch factor for fields that pass the couch either proximal or distal to the patient as couch absorption will cause an

underestimation of patient dose if not accounted for. The EPIgray algorithm deals with this through application of an average couch factor to all fields. If a couch specific model is used within the TPS (as for IMRT patients at our centre) then care must be taken to ensure that EPIgray does not perform an additional couch attenuation correction. However for 3D conformal patients at our centre no TPS couch model is implemented (with manual correction for couch transmission applied to field MU) and so the EPIgray couch factor was applied. This average factor will cause an overestimate to lateral fields that do not traverse the couch, and an underestimate of oblique fields that traverse a greater thickness of couch, on the order of $\pm 1\%$.

We have developed a decision tree for clinical workflow of EPIgray (Figure 8). If fields fell outside of the set tolerance ($\%\Delta D \pm 5\%$ in this trial instance) an investigation was conducted by the radiotherapy physics department to find the reason for the difference. The final investigation in Figure 8 is undertaken to investigate any potential patient anatomical changes such as bowel gas, weight loss / gain, and bladder filling that may have contributed to a discrepancy in reconstructed

dose.   Any   fields   that   fail   on   the   first   repeat   were   re-measured   using   diodes.
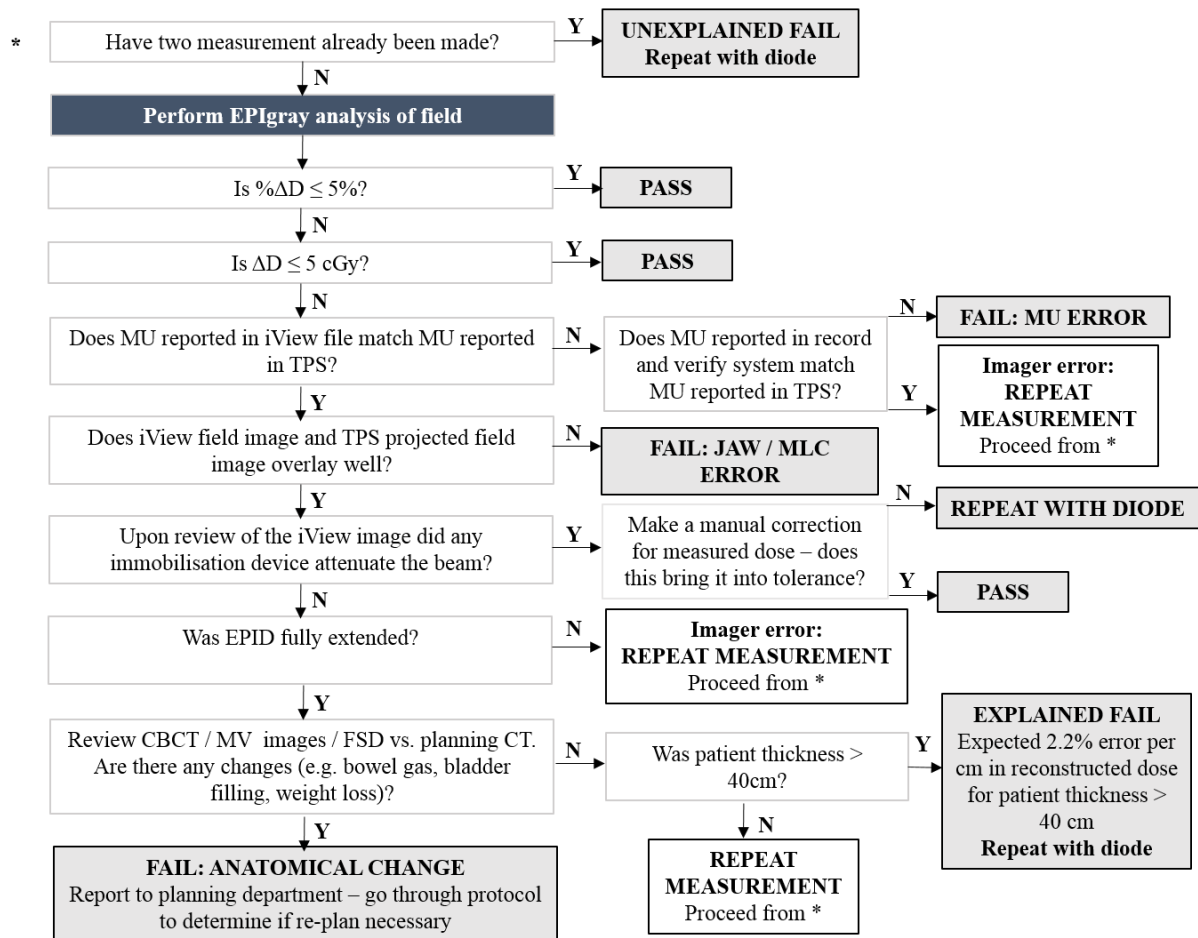


```
*        Have two measurement already been made? ──Y──▶  UNEXPLAINED FAIL
                          │                              Repeat with diode
                          │N
                          ▼
              Perform EPIgray analysis of field

              Is %ΔD ≤ 5%? ──Y──▶ PASS
                          │N
                          ▼
              Is ΔD ≤ 5 cGy? ──Y──▶ PASS
                          │N
                          ▼
  Does MU reported in iView file match MU reported ──N──▶ Does MU reported in record ──N──▶ FAIL: MU ERROR
  in TPS?                                                  and verify system match
                          │Y                               MU reported in TPS? ──Y──▶ Imager error:
                          ▼                                                            REPEAT
  Does iView field image and TPS projected field ──N──▶ FAIL: JAW / MLC               MEASUREMENT
  image overlay well?                                    ERROR                         Proceed from *
                          │Y
                          ▼
  Upon review of the iView image did any ──Y──▶ Make a manual correction ──N──▶ REPEAT WITH DIODE
  immobilisation device attenuate the beam?      for measured dose – does
                          │N                      this bring it into tolerance? ──Y──▶ PASS
                          ▼
  Was EPID fully extended? ──N──▶ Imager error:
                          │Y       REPEAT MEASUREMENT
                          ▼        Proceed from *
  Review CBCT / MV images / FSD vs. planning CT. ──N──▶ Was patient thickness > ──Y──▶ EXPLAINED FAIL
  Are there any changes (e.g. bowel gas, bladder         40cm?                          Expected 2.2% error per
  filling, weight loss)?                                  │N                             cm in reconstructed dose
                          │Y                              ▼                              for patient thickness >
                          ▼                          REPEAT                             40 cm
  FAIL: ANATOMICAL CHANGE                            MEASUREMENT                        Repeat with diode
  Report to planning department – go through protocol Proceed from *
  to determine if re-plan necessary
```

Figure 8 Flow chart of clinical investigation workflow for out of tolerance results.

Transit dosimetry is a sound final step in the treatment chain with potential to determine errors in dose delivery, without additional dose to the patient or time demands. It is beneficial that the commercial software allowed flexibility in dose calculation point location, but a full 2D map of TPS – transit dose discrepancy would be of greater use in providing more insight into not only location but distribution of the error source. A new software feature enables calculation of the gamma value [23] of the dose reconstruction point P across a local area of 30-mm centered around P for each field, comparing D_{EPI} at P to the TPS dose map (dose agreement and distance to agreement criterion can be manually set by the user). We are currently assessing this feature for our IMRT patients. Analysis was performed offline, but the ultimate goal would be to spot

errors in real-time to reduce the impact of severe errors. The software algorithm used the planning CT to reconstruct the patient dose; for a true in vivo dosimetry measurement this should be performed using CBCT information acquired on-set such that dose is reconstructed on current patient geometry. However, it was not the primary goal of this technique to record in vivo doses, but to identify errors, and for this aim the planning CT was the ideal choice of patient information to magnify the impact of anatomical changes between the planning and treatment stages.

5 Conclusions

A commercially available system for patient dose verification was implemented and tested with a series of phantom and patient measurements. Commissioning was simple and implementation measurements were not excessive and could be performed in 5 hours with an additional 2-3 hours per linac. The commercial system was used to verify 126 3D conformal beams delivered to a cohort of 37 patients. The preliminary data suggested that difference action levels may be required for different treatment sites. Patient positioning errors could be spotted by this system. False positive errors were due to algorithm limitation, EPID imager malfunction, and attenuation of the exit beam through immobilisation devices. Through using an appropriate clinical workflow for investigation of out of tolerance results, true positives can be recognised from false positives, and thus real dose delivery errors can be minimised.

6 Acknowledgments

7 References

[1] Van Dam, J and Marinello G. Methods for in vivo dosimetry in external radiotherapy. ESTRO 2006;2nd editio.

[2] Yorke E, Alecu R, Fontenla D, Ding L, Kalend A, Kaurin D et al. Diode in vivo dosimetry for patients receiving external beam radiotherapy: recommendations of the AAPM radiation therapy committee. Task Gr 62, Med Phys Publ 2005.

[3] The Royal College of Radiologists, Society and College of Radiographers, IPEM, National Patient Safety Agency BI of R. Towards Safer Radiotherapy 2008.

[4] Royer P, Marchesi V, Rousseau V, Buchheit I, Wolf D, Peiffert D, et al. Evaluation of transit in vivo dosimetry using portal imaging and comparison with measurements using diodes. Cancer / Radiother 2014;18:183–90. doi:10.1016/j.canrad.2014.03.006.

[5] Gierga DP, Brewer J, Sharp GC, Betke M, Willett CG, Chen GTY. The correlation between internal and external markers for abdominal tumors: Implications for respiratory gating. Int J Radiat Oncol Biol Phys 2005;61:1551–8. doi:10.1016/j.ijrobp.2004.12.013.

[6] Juhler Nøttrup T, Korreman SS, Pedersen AN, Aarup LR, Nyström H, Olsen M, et al. Intra- and interfraction breathing variations during curative radiotherapy for lung cancer. Radiother Oncol 2007;84:40–8. doi:10.1016/j.radonc.2007.05.026.

[7] Warkentin B, Steciw S, Rathee S, Fallone BG. Dosimetric IMRT verification with a flat-panel EPID. Med Phys 2003;30:3143–55. doi:10.1118/1.1843471.

[8] van Elmpt W, McDermott L, Nijsten S, Wendling M, Lambin P, Mijnheer B. A literature review of electronic portal imaging for radiotherapy dosimetry. Radiother Oncol 2008;88:289–309. doi:10.1016/j.radonc.2008.07.008.

[9] Steciw S, Warkentin B, Rathee S, Fallone BG. Three-dimensional IMRT verification with a flat-panel EPID. Med Phys 2005;32:600–12. doi:10.1118/1.1843471.

[10] McCurdy BMC. Dosimetry in radiotherapy using a-Si EPIDs: Systems, methods, and applications focusing on 3D patient dose estimation. J Phys Conf Ser 2013;444:012002. doi:10.1088/1742-6596/444/1/012002.

[11] Mans A, Wendling M, McDermott LN, Sonke J-J, Tielenburg R, Vijlbrief R, et al. Catching errors with in vivo EPID dosimetry. Med Phys 2010;37:2638–44. doi:10.1118/1.3397807.

[12]   Kavuma A, Glegg M, Currie G, Elliott A. Assessment of dosimetrical performance in 11 Varian a-Si-500 electronic portal imaging devices. Phys Med Biol 2008;53:6893–909. doi:10.1088/0031-9155/53/23/016.

[13]   McCurdy BMC, Greer PB. Dosimetric properties of an amorphous-silicon EPID used in continuous acquisition mode for application to dynamic and arc IMRT. Med Phys 2009;36:3028–39. doi:10.1118/1.3148822.

[14]   Nijsten SMJJG, Minken AWH, Lambin P, Bruinvis IAD, Minken) A W H. Verification of treatment parameter transfer by means of electronic portal dosimetry. Med Phys Med Phys 2004;31. doi:10.1118/1.1640972.

[15]   Nijsten SMJJG, Mijnheer BJ, Dekker ALAJ, Lambin P, Minken AWH. Routine individualised patient dosimetry using electronic portal imaging devices. Radiother Oncol 2007;83:65–75. doi:10.1016/j.radonc.2007.03.003.

[16]   Pasma KL, Kroonwijk M, Quint S, Visser AG, Heijmen BJM. Transit dosimetry with an electronic portal iaging device (EPID) for 115 prostate cancer patients. Int J Radiat Oncol Biol Phys 1999;45:1297–303.

[17]   Cilla S, Azario L, Greco F, Fidanzio A, Porcelli A, Grusio M, et al. An in-vivo dosimetry procedure for Elekta step and shoot IMRT. Phys Medica 2014;30:419–26. doi:10.1016/j.ejmp.2013.11.005.

[18]   Francois P, Boissard P, Berger L, Mazal A. In vivo dose verification from back projection of a transit dose measurement on the central axis of photon beams. Phys Medica 2011;27:1–10. doi:10.1016/j.ejmp.2010.06.002.

[19]   Elekta Limited. Elekta IviewGT. Corrective maintenance manual 2006.

[20]   Winkler P, Hefner A, Georg D. Implementation and validation of portal dosimetry with an amorphous silicon EPID in the energy range from 6 to 25 MV. Phys Med Biol 2007;52:N355–65. doi:10.1088/0031-9155/52/15/N05.

[21]   Boissard P, Franç Ois P, Rousseau V, Mazal A. Évaluation et mise en oeuvre de la dosimétrie in vivo de transmission par imageurs portals Evaluation and implementation of in vivo transit dosimetry with EPID. Cancer / Radiother 2013;17:656–63. doi:10.1016/j.canrad.2013.03.009.

[22]   D I Thwaites, J R Williams, E G Aird, S C Klevenhagen PW. A dosimetric intercomparison of megavoltage photon beams in UK radiotherapy centres. Phys Med Biol 1992;37:445–61.

[23]   Low DA, Harms WB, Mutic S, Purdy JA. A technique for the quantitative evaluation of dose distributions. Med Phys Med Phys 1998;25. doi:10.1118/1.1446110.